

# An efficient computational method for the implementation of a semi-classical instanton approach using discretized path integrals

著者	Kawatsu T., Miura Shinichi
journal or publication title	Journal of Physics: Conference Series
volume	454
number	1
page range	12030
year	2013-01-01
URL	<a href="http://hdl.handle.net/2297/36258">http://hdl.handle.net/2297/36258</a>

doi: 10.1088/1742-6596/454/1/012030

# An efficient computational method for the implementation of a semi-classical instanton approach using discretized path integrals

T Kawatsu<sup>1,2,\*</sup> and S Miura<sup>2,\*</sup>

<sup>1</sup>Institute for Molecular Science, National Institute of Natural Science, 38 Nishigonaka, Myodaiji, Okazaki 222-8585, Japan

<sup>2</sup>Graduate School of Natural Science and Technology, Kanazawa University, Kakuma, Kanazawa 920-1192, Japan

\*E-mail: kawatsu@fukui.kyoto-u.ac.jp, smiura@mail.kanazawa-u.ac.jp

**Abstract.** In the present paper, a numerical method for a semi-classical instanton method was examined. We implemented the instanton approach using discretized path integrals. The computational accuracy of the method is controlled by the following two parameters: the imaginary time duration ( $\tau$ ) and the time increment ( $\Delta\tau$ ), which represents the discretized path integral. To obtain accurate results, a long  $\tau$  must be used in combination with a short  $\Delta\tau$ ; however, because the computational cost is virtually proportional to  $\tau/\Delta\tau$ , the instanton calculations were computationally expensive under these conditions. In the present study, we propose a method that reduces the computational cost and represents long  $\tau$  instanton trajectories by employing an extended instanton trajectory from calculations based on a short  $\tau$ . We applied the method to calculate tunnel splitting in a HO<sub>2</sub> hydrogen transfer reaction using the double many-body extension IV potential as a validation.

## 1. Introduction

A useful method of analyzing chemical reactions is the intrinsic reaction coordinate (IRC), which is a minimum energy path connecting an initial state to a final state in the configurational space of target systems. When quantum mechanical fluctuations are important for describing molecular processes, the description of chemical processes must be improved from a simple IRC. For example, a reaction path Hamiltonian method provides a theoretical tool that describes quantum mechanical processes on the basis of the IRC [1]. Nevertheless, Carrington Jr. and Miller have reported that the reaction pathway of intra-molecular hydrogen transfer in a malonaldehyde molecule deviates from the IRC due to tunneling effects [2]. To represent molecular processes affected by tunneling, the aforementioned authors developed a reaction surface Hamiltonian approach where two reaction coordinates are adopted to describe large amplitude motions that cannot be represented by the reaction path Hamiltonian approach. The reaction surface Hamiltonian approach provides useful tools and a rigid theoretical basis; however, the reaction coordinates must be pre-defined, which may be difficult for multi-dimensional systems. In such cases, path integral methods can be effectively applied because all of the degrees of freedom can be treated equally. Approaches based on path integral Monte Carlo [3] and molecular dynamics [4] can yield numerically exact results for molecular processes without pre-defined reaction coordinates. However, these methods require massive samplings to calculate highly quantitative tunnel effects, and many tunneling pathways must be included. As a result, the

computational cost of these methods is rather expensive. In contrast, the instanton approach [5-10] in path integral theory, which is classified as a Wentzel-Kramers-Brillouin type approximation in standard quantum mechanics, is based on a semi-classical method and can be applied to a path integral representing tunneling effects. In the instanton approach, the instanton trajectory is determined to minimize the action for the duration of the imaginary time. Harmonic fluctuations along the instanton trajectory are included analytically. Katsnelson et al. proposed a method to determine the instanton trajectory by directly solving the imaginary time Newtonian equation [7]. In contrast, Mil'nikov and Nakamura determined the instanton trajectory by optimizing the action of the path [8,9]. Following the work of Mil'nikov and Nakamura, Richardson and Althorpe implemented the instanton approach using a discretized path integral representation [10]. Because the discretized path integral representation method has been used extensively in path integral Monte Carlo and molecular dynamics, the well-tested algorithms used in the aforementioned calculations can be used to develop the code for instanton calculations. Here, we briefly describe the Richardson-Althorpe instanton approach [10].

In the path integral theory, a propagator between the initial ( $q^{(1)}$ ) and final ( $q^{(M+1)}$ ) states is written as Equation (1), using a second order Suzuki-Trotter formula [10]:

$$G(q^{(1)}, q^{(M+1)}; \tau) \equiv \left\langle q^{(1)} \left| e^{-\frac{\hat{H}\tau}{\hbar}} \right| q^{(M+1)} \right\rangle = \left( \frac{1}{2\pi\hbar\Delta\tau} \right)^{\frac{3NM}{2}} \int dq^{(2)} \dots dq^{(M)} e^{-\frac{1}{\hbar}S(q^{(1)}, \dots, q^{(M+1)})}, \quad (1)$$

and

$$S(q^{(1)}, \dots, q^{(M+1)}) = \sum_{n=1}^M \frac{\Delta\tau}{2} \left( \frac{q^{(n)} - q^{(n+1)}}{\Delta\tau} \right)^2 + \sum_{n=2}^M \Delta\tau V(q^{(n)}) + \frac{\Delta\tau}{2} (V(q^{(1)}) + V(q^{(M+1)})), \quad (2)$$

where  $\tau$  is an imaginary time duration from  $q^{(1)}$  to  $q^{(M+1)}$ ,  $\Delta\tau$  is an interval between adjacent imaginary time slices, and  $N$  is the number of atoms in the original system. The total number of time slices is expressed as  $M \equiv \tau/\Delta\tau$ ,  $\hat{H}$  is the Hamiltonian, and  $q^{(n)}$  is the set of mass-weighted Cartesian coordinates of the original system at imaginary time slice  $n$ . Equations (1) and (2) can be interpreted as a configurational integral of classical polymers with a potential function  $S/\tau\hbar$ , where each polymer consists of  $N$  interaction sites or beads. Snapshots or replicas of the system at adjacent imaginary time slices are connected by harmonic springs. Interatomic interaction at each time slice is expressed as  $V(q^{(n)})$  ( $n=2, \dots, M$ ) and  $V(q^{(n)})/2$  ( $n=1, M+1$ ). In the instanton approach, instead of integrating the entire  $\{q^{(n)}\}$  space (= integrating all paths connecting from  $q^{(1)}$  to  $q^{(M+1)}$ ), we evaluate a stationary phase contribution by applying the following conditions:  $\partial S/\partial q^{(n)} = 0$ , which gives the instanton trajectory or optimized configuration of the polymer and includes its surrounding harmonic fluctuation. Path integral theory suggests that such a path (namely, the classical solution) has more possibilities than other paths. This approximation significantly reduces the computational cost compared to sampling approaches such as path integral Monte Carlo or molecular dynamics simulations yet still includes the harmonic component of quantum fluctuations along the instanton trajectory. Although an instanton with a single transition is determined, the pathway that goes back and forth many times also provides a stationary phase contribution, which can be included analytically by neglecting correlations among transitions. The action along the instanton trajectory is denoted as  $S_{inst}$ . Tunnel splitting ( $\Delta\epsilon$ ) is then expressed in accordance with the results described in the literature [10]:

$$\Delta\epsilon = \lim_{\tau \rightarrow \infty} 2\hbar K e^{-S_{inst}/\hbar}, \quad (3)$$

$$K \equiv \sqrt{\frac{S_{inst}}{2\pi\hbar}} \Phi^{-1}, \quad (4)$$

and

$$\Phi \equiv \left( \frac{\det' J_{inst}}{\det J_0} \right)^{\frac{1}{2}}, \quad (5)$$

where  $K$  is a coefficient that counts contributions from harmonic fluctuations around the instanton trajectory,  $J_{inst}$  and  $J_0$  are  $3MN \times 3MN$  Hessian matrices of the instanton trajectory and the trajectory that all time slices remain on in either the initial or final state, respectively. The Hessian  $J_{inst}$  has one zero eigenvalue associated with the translation of the instanton trajectory in imaginary time, and  $\det'$  indicates the determinant without a zero eigenvalue mode.

In the present study, we adopted the Richardson-Althorpe approach for instanton calculations. Possible improvements to their computational methods were also examined. First, we investigated the effect of  $\Delta\tau$  on the evaluation of  $S_{inst}$  and  $\Phi$  for a given value of  $\tau$ . Next, we determined the dependence on  $\tau$  in the tunnel splitting calculation. We then proposed an efficient method of extending  $\tau$  to reduce the computational cost and maintain accuracy. Section 2 includes the computational results and a brief discussion. In subsection 2.1, we show a computational result of the instanton trajectory and tunnel splitting for hydrogen transfer in a  $\text{HO}_2$  molecule using a double many-body extension (DMBE) IV potential [11]. In subsection 2.2, the parameter dependences of systematic errors on the instanton action and tunnel splitting are discussed. In section 2.3, we propose a method to efficiently extend  $\tau$ . Section 3 includes a summary of our results.

## 2. Results and discussions

### 2.1. $\text{HO}_2$ hydrogen transfer pathway

To examine the usefulness of the method, we applied the instanton approach to hydrogen transfer in a molecule of  $\text{HO}_2$ . This system has been well studied and is considered a benchmark molecular system [8-10]. In accordance with prior research [8-10], we employed the DMBE IV empirical potential field [11]. The instanton trajectory was obtained by optimizing action Equation (2) using the L-BFGS method [12]. To diagonalize Hessians, LAPACKE in Intel MKL library was employed. In the course of the optimization, both ends of the instanton trajectory were considered to be movable to exclude the overall rotation and translation between initial and final coordinates. In Figure 1, the computed instanton trajectory and IRC trajectory are drawn on the potential surface. The angle  $\gamma$  indicates the progress of hydrogen transfer from one oxygen to the other. The O-O distance ( $r_{OO}$ ) represents collective heavy atomic motion ( $r_{cH}$ ), which is the distance between the hydrogen atom and the center of the oxygen pair, and helps to represent hydrogenic motion with an angle of  $\gamma$ . Figure 1a shows that the instanton trajectory represented by  $r_{OO}$  and  $\gamma$  deviates from the IRC. The characteristic difference between the instanton and the IRC is the motion of oxygen. In the IRC, the O-O bond stretches when the system approaches the potential barrier, which leads to a relatively low potential barrier. In contrast to the IRC, the instanton pathway is primarily constructed based on the motion of hydrogen. Because the instanton corresponds to tunnel transfer, heavy atoms are much less active than light atoms. The instanton goes over a higher potential barrier than the IRC due to the tunneling effect. Figure 1b primarily shows hydrogenic motion because the center of the oxygen pair remains nearly constant during the hydrogen transfer reaction. Subsequently, both the IRC and instanton trajectories draw curves that are close to each other on a plane by the coordinates  $r_{cH}$  and  $\gamma$ . The computed value of tunnel splitting was  $\Delta\epsilon=7.0 \times 10^{-9} \text{ cm}^{-1}$ , which is in agreement with Richardson's prior calculation [10].

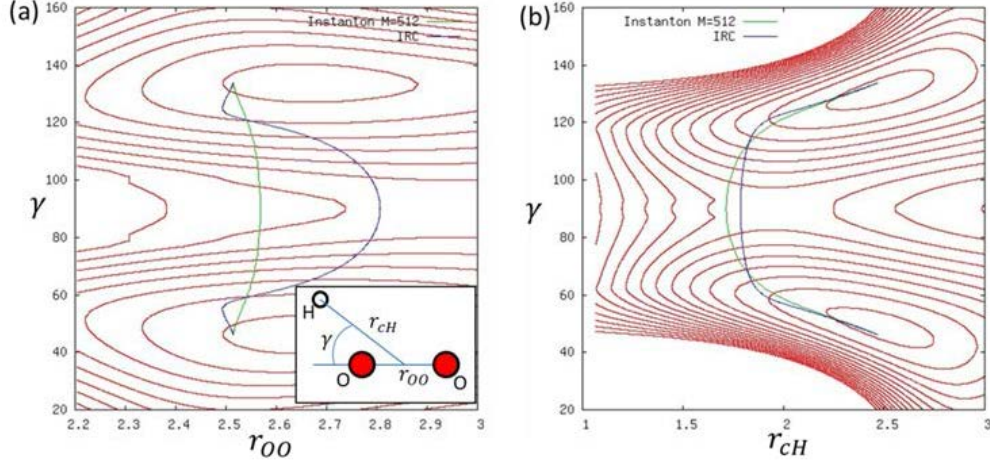


Figure 1. Instanton and IRC trajectories for HO<sub>2</sub> hydrogen transfer. Green and blue curves represent the instanton and IRC, respectively. Red curves are contour lines of the potential surface. The parameters  $\tau=3600$  and  $M=512$  were applied. Axis notations are described in the inset of Figure 1a.

## 2.2. Parameter dependences of systematic errors

We first present the systematic errors on the numerical values of  $S_{inst}$  and  $\Phi$  that arise from the discretized approximation of the path integral. Due to the second order Suzuki-Trotter decomposition, the systematic error of the action of  $S_{inst}$  and  $\Phi$  will be proportional to  $\Delta\tau^2$  for a given  $\tau$ . Because the convergence of  $S_{inst}$  and  $\Phi$  with respect to  $\Delta\tau$  also depends on  $\tau$ , we must use a sufficiently large value of  $\tau$ , as shown in Equation (3). Figure 2a shows the corresponding proportions for various values of  $\tau$ . As shown in the figure, when  $\tau$  is greater than or equal to 1800 au, a single line is observed. However, when  $\tau=1200$  and 1800 au, the values are present in different series. This disagreement arises from the fact that the imaginary time duration is not large enough to represent the instanton trajectory connecting the initial and final configurations. A representative reaction coordinates  $\gamma$  at each imaginary time slice  $n\Delta\tau$  are presented in Figure 3a. The reaction coordinates  $\gamma$  with  $\tau=1200$ , 2400, 4800, and 9600 au are over-written in the figure. In the case of  $\tau=1200$  au, the configurations at both ends of the imaginary time duration  $\tau$  do not reach the initial and final configurations, respectively. In Figure 3a, the time for the transition from the initial to final configuration is estimated to be approximately 2000 au, which is the minimum duration of time ( $\tau$ ) required to converge  $S_{inst}$  in the present system. Thereafter, we adopted only results with  $\tau$  greater than 1800 au to avoid the aforementioned problem. Figure 2b presents  $\Delta\tau^2$  dependences for errors of  $\Phi$ , which is another factor that affects tunnel splitting. The error of  $\Phi$  was also proportional to  $\Delta\tau^2$ ; however, the calculated values converge more slowly on  $\tau$  compared to  $S_{inst}$ . The  $\Phi$  value is determined by the ratio of eigenvalues for  $J_{inst}$  and  $J_0$  in Equation (5). When  $\tau$  lengthens, the eigenvalues can change even though the transition region from the initial to the final configurations is identical. Because the values of  $\Phi$  obtained from  $\tau=14400$  and 19200 au were similar,  $\tau$  must be set to at least 14000 au to obtain an exact value of  $\Delta\epsilon$ . This value of  $\tau$  is much longer than that used to represent  $S_{inst}$ , and the computational cost is high.

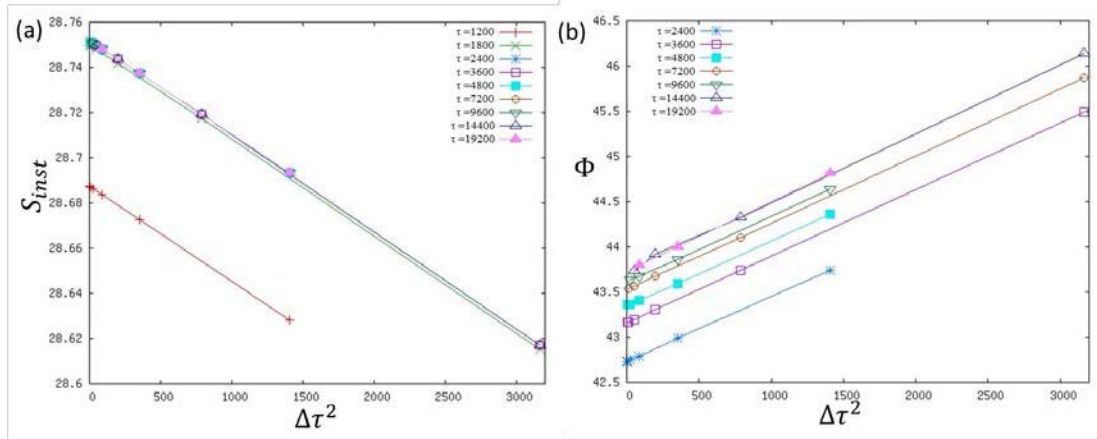


Figure 2.  $\Delta\tau^2$  dependences of systematic errors on (a)  $S_{inst}$  and (b)  $\Phi$  with various values of  $\tau$ .

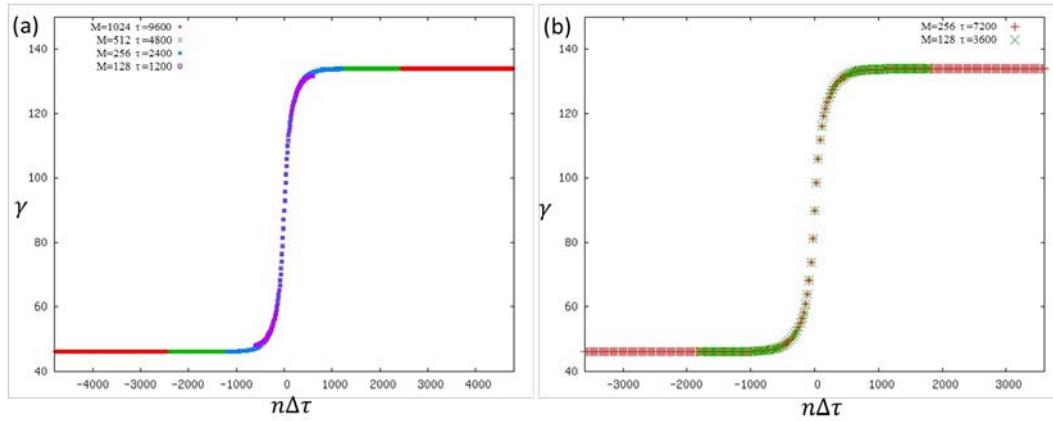


Figure 3. Representative reaction coordinates ( $\gamma$ ) at each imaginary time slice  $n\Delta\tau$  in the instanton trajectory. (a)  $\Delta\tau=9.375$  with short to long  $\tau$  parameters:  $\tau=1200$  (purple), 2400 (blue), 4600 (green), and 9600 (red). (b)  $\Delta\tau=28.125$  with two medium  $\tau$  parameters:  $\tau=3600$  (green) and 7200 (red). The horizontal axis  $\gamma$  is described in Figure 1.

### 2.3. Extension of the polymer length $\tau$

In Figure 3b, the reaction coordinates  $\gamma$  at each imaginary time slice  $n\Delta\tau$  were obtained with parameters  $\tau=3600$  or 7200 au and  $\Delta\tau=28.125$  au. Comparing these two calculations, the reaction coordinates  $\gamma$  at each time slice on the instanton are identical. Therefore, the differences caused by  $\tau$  come from the difference in the number of time slices at the initial and final configurations. These results suggest that we can add time slices at the initial and final configurations to both ends of the instanton trajectory to extend  $\tau$  without re-calculating the stationary phase for high values of  $\tau$ . When the configurations at both ends of the imaginary time duration  $\tau$  reach the initial and final configurations, respectively, Equation (2) predicts that the  $\tau$  extension does not affect  $S_{inst}$ . However,  $\Phi$  value depends on the  $\tau$  extension of the trajectory. The convergence for  $\tau$  value requests at least 14000 au as estimated in previous section. For example, if we can calculate  $\Phi$  value at  $\tau=19200$  au using the instanton trajectory optimized at  $\tau=3600$ , the size of the optimized system is four times smaller than fully optimized trajectory, because using the same  $\Delta\tau$ , the number of imaginary time slices  $M$  are proportional to  $\tau$ . The computational cost for the optimization reduces four times or more. In addition, we can also reduce the computational cost to calculate interatomic potential for added imaginary time slices by the  $\tau$  extension because these slices are the same as the initial or final geometries.

Figure 4 shows the computed values of (a)  $S_{inst}$  and (b)  $\Phi$  using the fully optimized calculations (horizontal axis) and the extension of  $\tau$  without re-optimization of the instanton trajectory (vertical axis). Superscript \* indicates the  $\tau$  extension results.  $S_{inst}^*$  is in agreement with the  $S_{inst}$  values shown in Figure 4a. In Figure 4b, the  $\tau$  extension results ( $\Phi^*$ ) also agree with the original  $\Phi$  values, except when  $\tau=2400$  au. These results demonstrate that we can extend  $\tau$  without re-optimizing the instanton trajectory obtained with a short  $\tau$ . We remark that  $\tau$  must not be too short. Namely,  $\tau=2400$  au is not long enough to provide a correct instanton trajectory, and the  $\tau$  extension process may expand the error.  $\Phi$  is computed using Hessians, and such calculations appear to be more sensitive to the accuracy of computational conditions. As shown in Figure 4b, numerical convergence on  $\Phi$  is achieved for  $\tau$  equal to or greater than 3600 au, which is approximately twice as long as the transition time estimated above. Thus, to obtain sufficient numerical accuracy with the  $\tau$  extension method, the optimized result for the instanton trajectory for the imaginary time duration had to be two times greater than the transition time in this system. Although several small errors are observed in Figure 4b, these errors are caused by the instanton trajectory optimization error for determining the stationary phase in the current calculation level.

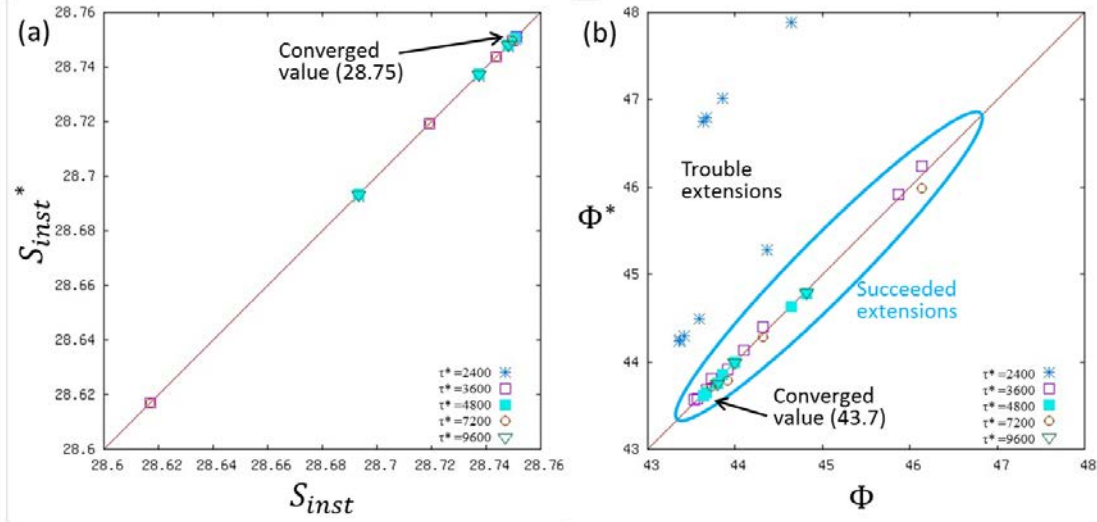


Figure 4. Accuracies of the extension of  $\tau$  for various  $\Delta\tau$  values for (a)  $S_{inst}$  and (b)  $\Phi$ . The horizontal axis is the fully optimized calculation, and the vertical axis is the extension of  $\tau$  without re-optimization.  $\tau^*$  indicates  $\tau$  before extensions. Pre-extended calculations are  $M=64$  ( $\tau^*=2400, 3600$ ), 128 ( $\tau^*=2400-7200$ ), 256 ( $\tau^*=2400-7200$ ), 512 (all  $\tau^*$ ), and 1024 (all  $\tau^*$ ) and all of these are extended to up to either  $M=2048$  or  $\tau=14400$  or 19200. The converged values are calculated by the least square fitting using results  $\tau=19200$  in Figure 2.

### 3. Concluding remarks

The instanton approach with the discretized path integral method can be directly applied to multi-dimensional systems. In the present paper, we proposed a method for efficient instanton calculations. The method reduces the computational cost associated with taking the long limit of  $\tau$ . In our method, the imaginary time duration  $\tau$  was extended by recycling the result of the converged instanton trajectory for a relatively short  $\tau$ . The numerical results presented in this paper indicated that our method produces accurate numerical values.

Similar to path integral Monte Carlo and molecular dynamics, interatomic interaction at each imaginary time slice can be calculated independently, and the instanton method can be easily implemented in highly parallel computational conditions with great efficiency. Additionally, the method presented in this paper can reduce computational costs; thus, we can invest these reduced computational costs to calculate the interatomic potential at each imaginary time slice using accurate quantum chemical calculations. These issues will be addressed in the near future.

## Acknowledgments

This work was partially supported by a Grant-in-Aid for Scientific Research (C) (No. 23550011) from the Japan Society for the Promotion of Science and by the Strategic Programs for Innovative Research (SPIRE), MEXT, and the Computational Materials Science Initiative (CMSI), Japan.

## References

- [1] Miller W H, Handy N C and Adams J E 1980 *J Chem Phys* **72** 99
- [2] Carrington Jr. T and Miller W H 1986 *J Chem Phys* **84** 4364
- [3] Tuckerman E M and Hughes A 1999 *Classical and Quantum Dynamics in Condensed Phase Simulations* ed G Ciccotti and D F Coker (Singapore: World Scientific) p. 311
- [4] Ceperley D M 1995 *Rev Mod Phys* **67** 279
- [5] Coleman S 1985 *Aspects of Symmetry* (New York, Melbourne: Cambridge University Press)
- [6] Altland A and Simons B 2006 *Condensed Matter Field Theory* (New York: Cambridge University Press)
- [7] Katsnelson M I, van Schilfgaarde M, Antropov V P and Harmon B N 1996 *Phys Rev A* **54** 4802
- [8] Mil'nikov G and Nakamura H 2008 *Phys Chem Chem Phys* **10** 1374
- [9] Mil'nikov G V and Nakamura H 2001 *J Chem Phys* **115** 6881
- [10] Richardson J O and Althorpe S C 2011 *J Chem Phys* **134** 054109
- [11] Pastrana M R, Quintales L A M, Brandão J and Varandas A J C 1990 *J Phys Chem-Us* **94** 8073
- [12] Nocedal J 1980 *Math Comput* **35** 773